An automatic early stage alveolar-bone-resorption evaluation method on digital dental panoramic radiographs

Min Zhang*[a], Akitoshi Katsumata[b], Chisako Muramatsu[a], Takeshi Hara[a], Hiroki Suzuki[b] and Hiroshi Fujita[a]

[a]Department of Intelligent Image Information, Division of Regeneration and Advanced Medical Sciences, Graduate School of Medicine, Gifu University, Gifu-Shi, 501-1194 Japan
[b]Department of Oral Radiology, School of dentistry, Asahi University, Gifu-Shi, 501-0296 Japan

ABSTRACT

Periodontal disease is a kind of typical dental diseases, which affects many adults. The presence of alveolar bone resorption, which can be observed from dental panoramic radiographs, is one of the most important signs of the progression of periodontal disease. Automatically evaluating alveolar-bone resorption is of important clinic meaning in dental radiology. The purpose of this study was to propose a novel system for automated alveolar-bone-resorption evaluation from digital dental panoramic radiographs for the first time. The proposed system enables visualization and quantitative evaluation of alveolar bone resorption degree surrounding the teeth. It has the following procedures: (1) pre-processing for a test image; (2) detection of tooth root apices with Gabor filter and curve fitting for the root apex line; (3) detection of features related with alveolar bone by using image phase congruency map and template matching and curving fitting for the alveolar line; (4) detection of occlusion line with selected Gabor filter; (5) finally, evaluation of the quantitative alveolar-bone-resorption degree in the area surrounding teeth by simply computing the average ratio of the height of the alveolar bone and the height of the teeth. The proposed scheme was applied to 30 patient cases of digital panoramic radiographs, with alveolar bone resorption of different stages. Our initial trial on these test cases indicates that the quantitative evaluation results are correlated with the alveolar-bone-resorption degree, although the performance still needs further improvement. Therefore it has potential clinical practicability.

Keywords: Panoramic radiograph, alveolar bone resorption, occlusion line, root apex, phase congruency, Gabor filter.

1. INTRODUCTION

Recently, digital panoramic scanners are rapidly spreading. Panoramic radiography has been an important component of dental diagnostic radiology for over 40 years. It is a technique that produces an image of the teeth and jaws on a single film, but it also depicts a somewhat bewildering array of hard and soft tissues in the head and neck. Findings in panoramic radiographs play an important role for diagnosis in dental clinics. It is generally widely accepted that radiographs supplement clinical examination in establishing the diagnosis and guiding the treatment plan for a patient affected by those periodontal diseases which have contributed to destruction of the periodontal attachment. A range of findings that have relevance to clinically evident periodontal conditions can become apparent on radiographs. Radiographs can provide key information of relevance to periodontal decision making which dentists are not capable to capture by clinical examination, such as a length of root(s) with remaining bony support.

Medical Imaging 2014: Computer-Aided Diagnosis, edited by Stephen Aylward, Lubomir M. Hadjiiski,
Proc. of SPIE Vol. 9035, 90353G · © 2014 SPIE · CCC code: 1605-7422/14/$18 · doi: 10.1117/12.2044348

Panoramic radiographs, which allow visualization of overall structures of dentoalveolar anatomy at low cost and relatively low radiation exposure, have been employed applied in clinical practice and research in dentistry. They have been used to qualitatively examine and evaluate dental caries, periradicular disease, maxillary impacted canines, mandibular impacted third molars, alveolar bone, etc.

Periodontal disease is a kind of typical dental diseases, which affects many adults. The presence of alveolar bone resorption is one of the most important signs of periodontal disease. In dental panoramic images the information on physical change of organs such as the alveolar bone and jaw bones is very important to diagnose several diseases. The panoramic radiograph is excellent for visualization of the progression of alveolar bone resorption.

Figure 1 (a) shows two examples of panoramic radiographs. The severe alveolar bone absorption (white arrows) are found in the upper and lower jaws of left molars. Figure 1 (b) shows the enlargement of panoramic X-ray image with periodontal disease. From Figure 1 (b) alveolar bone level can be seen in the X-ray image of teeth: The normal alveolar bone level in the dash line and the actual alveolar bone level in solid line. The panoramic radiograph is excellent for visualization of the progression of alveolar bone resorption. Detection of such signs on digital dental panoramic (DPR) radiograph has a potential to provide benefits for both patients and dentists. To assist such screening pathway, development of a computer aided diagnosis (CAD) system for the evaluation of such diseases using panoramic radiography is currently in progress.

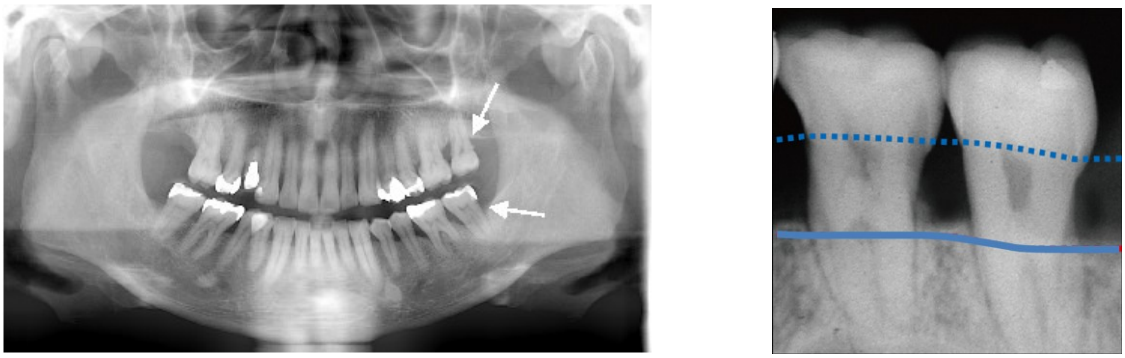

(a) (b)

Figure 1 (a) Panoramic X-ray image showing the periodontal disease (see the white arrow.). (b) Teeth periodontal disease: alveolar bone levels seen in the X-ray image.

2. METHOD

The purpose of this study is to propose a novel system for automatic alveolar-bone-resorption evaluation for digital panoramic radiographs. The general framework of the proposed method is shown in Figure 2. It has the following procedures: (1) pre-processing for a test image; (2) detection of teeth root apex with Gabor filter and curve fitting for the root apex line; (3) detection of feature related with alveolar bone by using image phase congruency (PC) map and curve fitting for the alveolar line; (4) detection of occlusion line with selected Gabor filter; (5) quantitative alveolar-bone-resorption degree evaluation.

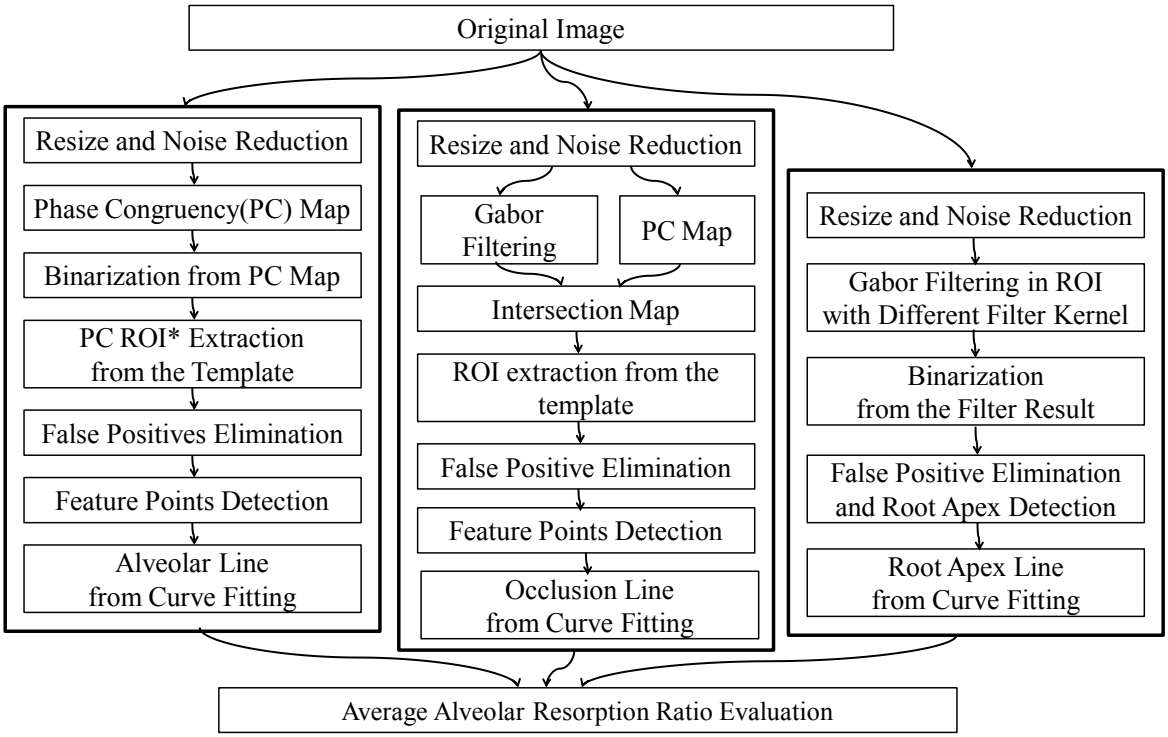

Figure 2 The general framwork for the proposed method.

The following sections include the details of the proposed system.

2.1 Preparation of the region of interest (ROI) mask

For the detection of reliable features for the occlusion line, root apex line and alveolar line, a ROI mask is necessary. The description of the usage of the ROI mask will be described in the following sections. As shown in Figure 3, for each DPR, the mandibular contour was extracted with the method proposed in [1]. Then the mandibular contour is shifted in the vertical orientation. The mask is produced by the enclosed area by the two mandibular contours. The general ROI template is created from the average map of a series of ROIs.

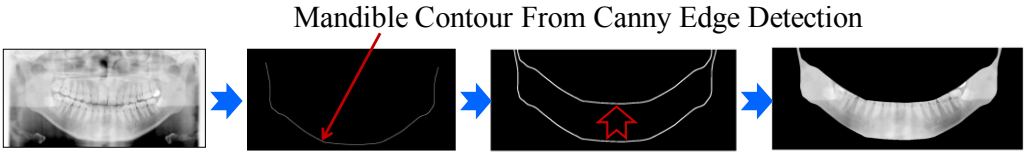

Figure 3 An example of ROI template extraction.

2.2 The detection of root apex line

The detection of root apex line is as follows.

(1) A test image is subsampled by the factor of 3 and cropped for the computational simplicity;

(2) Gabor filter [2, 3] is introduced for the detection of root apex. With Gabor filters, a test image is filtered with different Gabor filter kernels in ROI; the incisor area is ignored due to the low contrast.

Previously, a number of authors used a bank of Gabor filters to extract local image features. An input image $I(x,y), x, y \in \Omega$ (Ω represents a set of image points), is convolved with a two 2-dimentional Gabor function $g(x,y)$ to obtain a Gabor feature image $r(x,y)$. We use the following family of Gabor functions:

$$g_{\lambda,\theta,\varphi}(x,y) = e^{-\frac{(x'^2+\gamma^2 y'^2)}{2\sigma^2}} \cos(2\pi\frac{x}{\lambda}+\varphi) \tag{1}$$

$$x' = x\cos\theta + y\cos\theta$$
$$y' = -x\sin\theta + y\cos\theta$$

The standard deviation σ of the Gaussian factor determines the effective size of the surrounding of a pixel in which weighted summation takes place. The eccentricity of the Gaussian and here with the eccentricity of the convolution kernel g is determined by the parameter γ, called the spatial aspect ratio. The value γ is a constant. The angle parameter θ specifies the orientation of the normal to the parallel positive and negative lobes of the Gabor filters. The Gabor filter kernels used in this paper are shown in Figure 4.

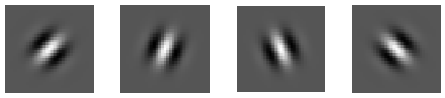

Figure 4 The different Gabor filter kernels used in different area.

(3) Then, the filtered image is binarized with a threshold;

(4) False positives are eliminated according to the area and position of the binary results;

(5) After false positive elimination, root apices are detected. Least squares regression for quadratic curve fitting (also referred to as non-linear or second order regression) is introduced for the root apex line detection. Figure 5 shows an example for the root apex line detection.

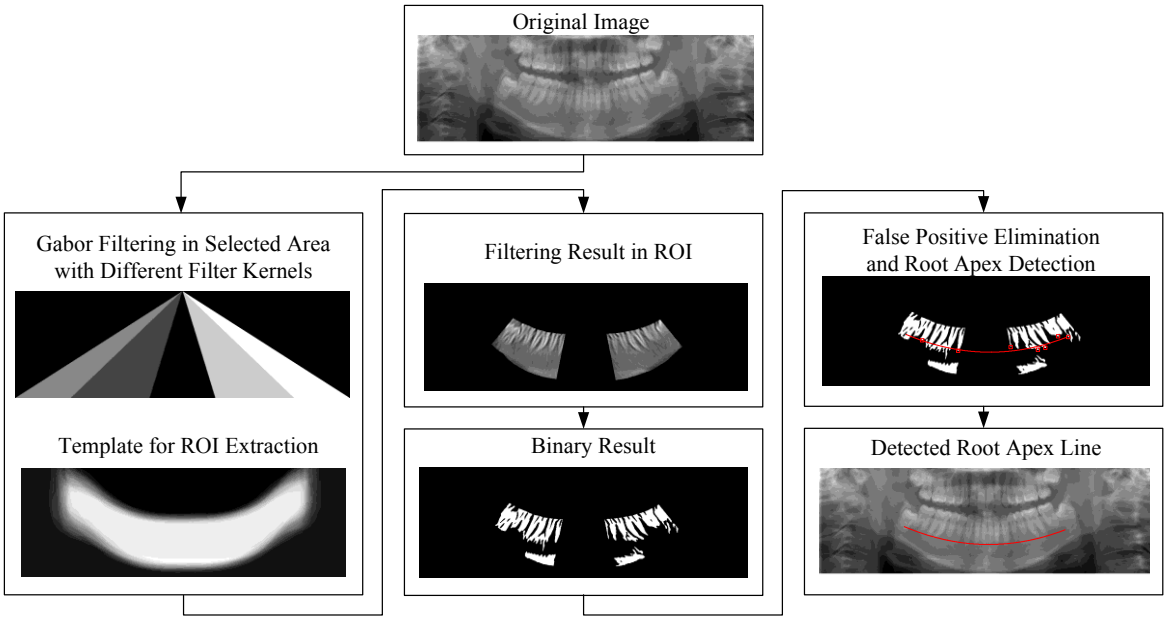

Figure 5 An example of the root apex line detection.

2.3 The detection of alveolar line

The detection of alveolar line is as follows.

(1) Image phase congruency map [4] is extracted from the test image;

To calculate 2-D PC of a given image, the image is first convolved with a bank of log-Gabor filters. Let the image denoted by $I(x,y)$, the even- symmetric filter and odd-symmetric filter at scale *n* and orientation *o* denoted by M_{no}^{e} and M_{no}^{o}, respectively. The responses of each quadrature pair of filters are a vector:

$$[e_{no}(x,y), o_{no}(x,y)] = [I(x,y) \otimes M_{no}^{e}, I(x,y) \otimes M_{no}^{o}], \tag{2}$$

where $\otimes$ is the convolution operator. From Equation (2), the amplitude of this response is given by

$$A_{no}(x,y) = \sqrt{e_{no}^{2}(x,y) + o_{no}^{2}(x,y)} \tag{3}$$

And phase is given by

$$PC_2(x,y) = \frac{\sum_o \sum_n W_o(x,y) \lfloor A_{no}(x,y) \Delta\Phi_{no}(x,y) - T_o \rfloor}{\sum_o \sum_n A_{no}(x,y) + \varepsilon} \tag{4}$$

where $\lfloor \ \rfloor$ denotes that the enclosed quantity is equal to itself if it is positive, and equal to zero otherwise ; $W_o(x,y)$ o is a measure of significance of frequency spread; ε is a small positive constant used to prevent division of zero; *To* is a quantity introduced to compensate image noise; and $\Delta\Phi_{no}(x,y)$ is a sensitive phase deviation function defined as

$$\Delta\Phi_{no}(x,y) = \cos(\phi_{no}(x,y) - \bar{\phi}_{no}(x,y)) - \left|\sin(\phi_{no}(x,y) - \bar{\phi}_{no}(x,y))\right| \tag{5}$$

MATLAB code for computing the 2-D phase congruency can be found in [5].

(2) Then, the binarization of the phase congruency map is undertaken;

(3) Thirdly, the alveolar feature is detected in the ROI template and false positives are eliminated according to the area and position of the binary results;

(4) Finally, curve fitting for the alveolar line is carried out with least squares regression. Figure 6 shows an example for the alveolar line detection.

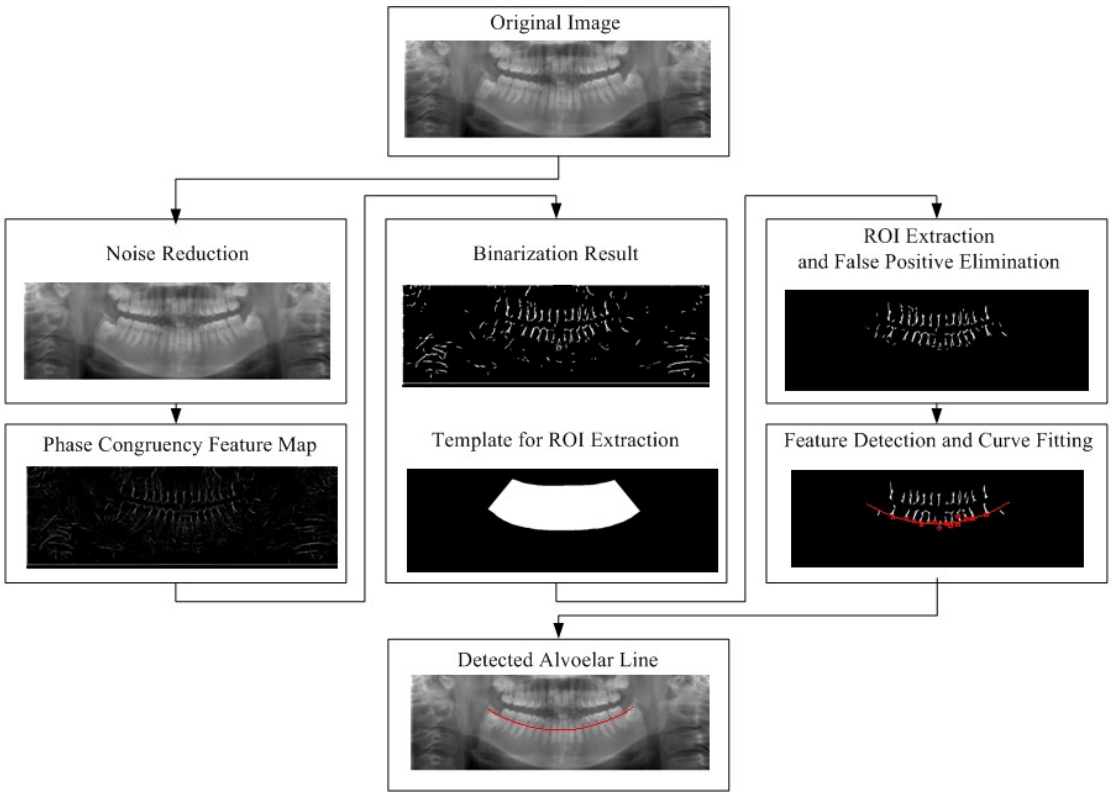

Figure 6 An example of the alvoelar line detection.

2.4 The detection of occlusion line

The detection of occlusion line is as followed.

(1) Horizontal Gabor filtering and binarization are performed for the input image;

(2) PC feature map is extracted for the input image;

(3) Intersection map between the binary map by Gabor filtering and PC map was created;

(4) Features in ROI template is extracted in panoramic radiograph;

(5) False positives are eliminated and curve fitting for the occlusion line is performed. Figure 7 shows an example of the occlusion line detection.

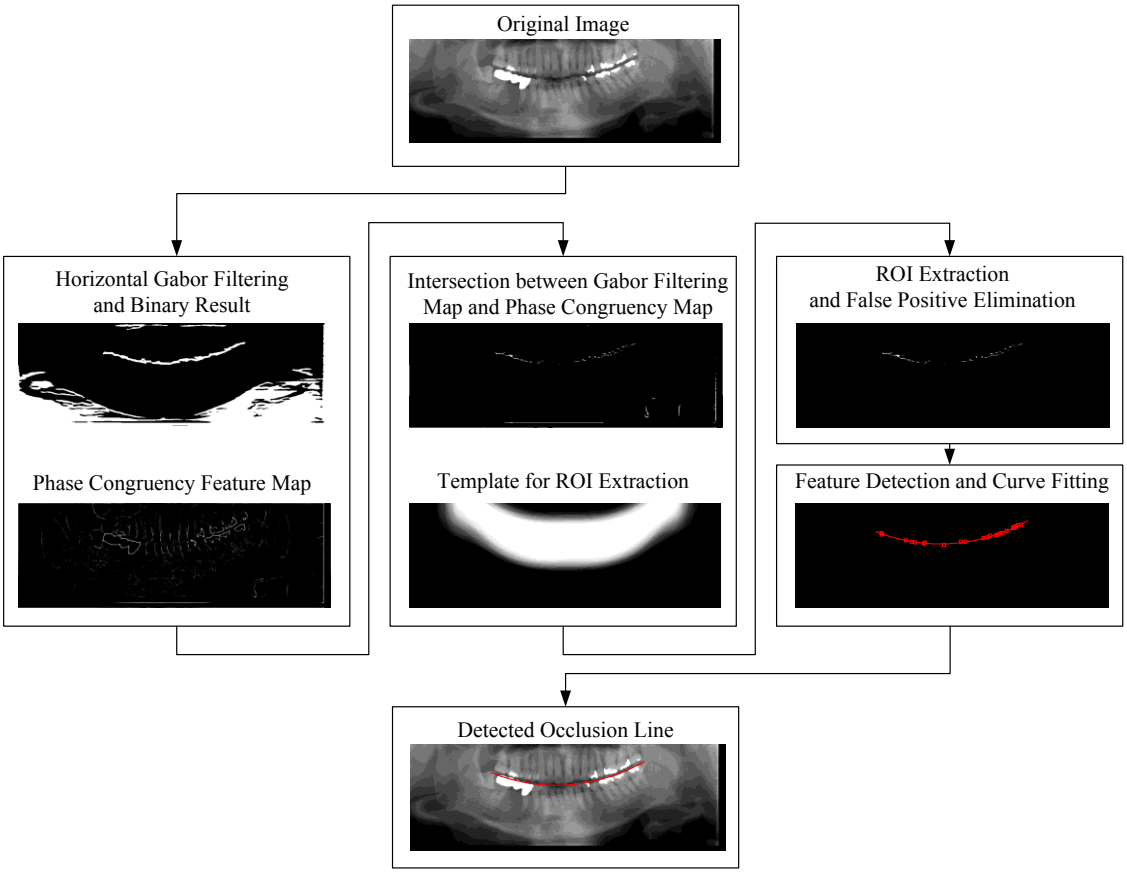

Figure 7 An example of the occlusion line detection.

3. EXPERIMENTS AND RESULTS

3.1 Data preparation

In the data acquisition, radiographic images were obtained at standard head positions using the new dental panoramic radiograph equipment- QRmaster-P^{TM} [6] (See Table 1). Our database consists of 30 panoramic images with different disease stages. These data are obtained at Asahi University Dental Hospital in Japan. The DPRs were taken with the standard positioning of the head such that the Frankfort horizontal plane was used as a reference line. The automatic mode was used to control the x-ray exposure.

Tables 1 and 2 show the detailed information about the data acquisition and the details of the number of test cases for each stage, respectively.

Table 1 Data acquisition information.

Generic name	Digital panoramic dental X-ray apparatus
Sales name	Telesytems Co Ltd, Osaka, Japan
Type	QRmaster-P^{TM} [6]
Format of Exported Image	JPEG, BMP, TIFF and PNG

Table 2 Details of test dataset.

	Normal	Mild	Moderate
No. of cases	17	11	2

3.2 Experimental results and comparison

In this section, we present the results of the proposed method. The preliminary experimental result is shown in Figure 8. Our initial trial on these test cases indicates that the quantitative evaluation results are correlated to the alveolar-bone-resorption degree.

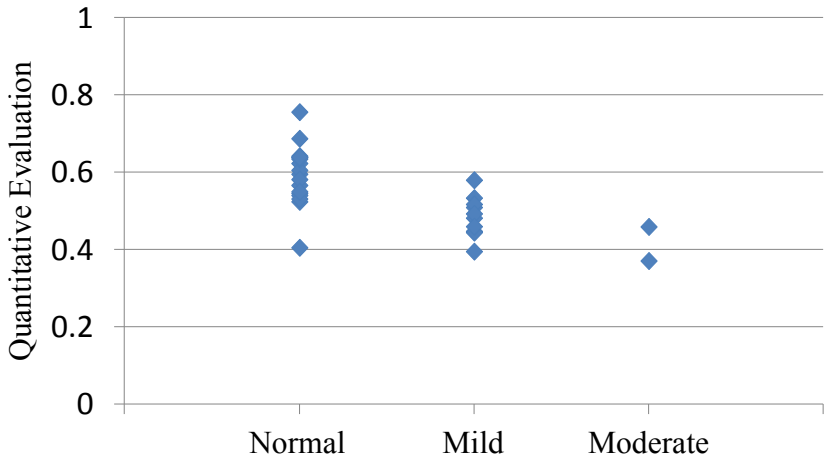

Figure 8. Quantitative evaluation results vs. the clinical diagnostic results.

4. CONCLUSION

We proposed a new system for automatically assessing alveolar bone resorption using digital panoramic radiographs. With this system, the alveolar-bone-resorption degree was automatically evaluated by the average ratio of the height of alveolar bone and the height of the teeth. Our initial trial on these test cases indicates that the quantitative evaluation results are correlated to the alveolar-bone-resorption degree, although the performance still needs further improvement. Therefore it may have potential clinical practicability.

ACKNOWLEGEMENT

The authors thank members of the Fujita Lab. in Gifu University for their valuable discussions. This study is supported in part by Strategic Information and Communications R&D Promotion Programme (SCOPE) by Ministry of Internal Affairs and Communications (MIC) Japan. The authors also gratefully acknowledge the Venture Business Laboratory (VBL) of Gifu University for the support of this research work.

REFERENCES

[1] T.Matsumoto, T.Hayashi, T.Hara, A.Katsumata, C.Muramatsu, X.Zhou, Y.Iida, M.Matsuoka, K.Katagi, and H.Fujita, "Automated scheme for measuring mandibular cortical thickness on dental panoramic radiographs for osteoporosis screening," Proc. SPIE Medical Imaging, Vol.8315, 83152L-1 - 83152L-6, (2012).

[2] C.J. Lee and S.D. Wang, "Fingerprint feature extraction using Gabor filters," Electronics Letters, Vol 35, No.4, 288–290, 1999.

[3] P. D. Kovesi, "Image features from phase congruency," J. Comput. Vis.Res., vol. 1, no. 3, Summer 1999.

[4] S. E. Grigorescu, N. Petkov, and P. Kruizinga, "Comparison of texture features based on Gabor filters," IEEE Trans. Image Processing, Vol. 11, pp. 1160–1167, Oct. 2002.

[5] P. D. Kovesi, MATLAB code for calculating phase con gruency and phase symmetry/asymmetry, April 1996. http://www.cs.uwa.edu.au/~pk/Research/research.html.

[6] http://www.telesystems.co.jp/dental/qrmaster_p/